Vol 11 No 7, July 2002
1009-1963/2002/11(07)/0694-06
Chinese Physics
© 2002 Chin. Phys. Soc.
and IOP Publishing Ltd

Photoionization properties of an atom with two autoionizing states*

Guo Hong(郭 红)†, Li Gao-Xiang(李高翔), and Peng Jin-Sheng(彭金生)

Department of Physics, Huazhong Normal University, Wuhan 430079, China

(Received 31 December 2001; revised manuscript received 1 April 2002)

We have investigated the photoionization properties of an atom with a ladder coupling scheme involving two autoionizing states coupled to each other. The effects of the coherent coupling between two autoionizing states and between the low-lying autoionizing state and the continuum on the ionization yield are discussed. The conditions leading to atomic coherent population trapping and the coherent population trapping states are given explicitly.

Keywords: photoionization, autoionizing state, coherent population trapping
PACC: 3280, 4250

1. Introduction

Coherent interactions between an atomic system with two electromagnetic fields in the so-called Λ, V and ladder coupling schemes have been the subject of a vast number of theoretical studies for many years. Because of the existence of the quantum interference effects in these atom–field coupling systems, several interesting and useful phenomena involving bound states and smooth or structured continua have been revealed theoretically and observed experimentally, such as laser-induced continuum structure,[1−9] atomic coherent population trapping,[10−14] electromagnetically induced transparency,[15−21] lasing without population inversion,[22,23] adiabatic population transfer,[24−26] and stabilization of Rydberg atom.[27−33] Karapanagioti *et al*[34,35] investigated the ionization properties of magnesium with a ladder coupling scheme involving two autoionizing states coupled to each other. The probing of the lower state through a weak electromagnetic field revealed strong modifications of the autoionizing line shape, depending on the detuning of the dressing field. They showed that the strong electromagnetic coupling of two autoionizing states can lead to a coherent population trapping of the fast-decaying probed autoionizing states, resulting in a reduction of ionization. Recently, Kylstra *et al*[36] studied the same system using the R-matrix Floquet theory. They have shown that, when the intensity of the laser is increased, the effect of an additional autoionizing state becomes significant.

In this paper, we focus our attention on the photoionization properties of an atom with a ladder coupling scheme involving two autoionizing states coupled to each other. In section 2, we give the model and the time evolution of the state vector of the system. Section 3 is devoted to the discussion of the effects of the coherent coupling between the two autoionizing states and between the low-lying autoionizing state and the continuum on the ionization yield. The line shape of the ionization yield versus the detuning of the transition between the ground state and the low-lying autoionizing state generally behaves as an asymmetric three-peak distribution, and in some special cases it is deteriorated to an asymmetric two-peak distribution similar to that in the standard Fano model.[37−39] The condition leading to atomic coherent population trapping and the coherent population trapping states is given explicitly. Finally, our conclusions are summarized in section 4.

2. Model and equation of motion

The atomic model, as shown in Fig.1, consists of three bound states $|j\rangle$ (j=1,2,3) with frequencies ω_j and a set of continuum states $\{|\varepsilon\rangle\}$, here the two bound states $|2\rangle$ and $|3\rangle$ are the autoionizing states which are embedded into the continuum $\{|\varepsilon\rangle\}$. The one-photon processes $|1\rangle \leftrightarrow |2\rangle$, $|1\rangle \leftrightarrow |\varepsilon\rangle$, $|2\rangle \leftrightarrow |3\rangle$ and $|2\rangle \leftrightarrow |\varepsilon\rangle$ are driven by two laser fields with frequencies ω_p and ω_d respectively. Unlike Ref.[7],

*Project supported by the National Natural Science Foundation of China (Grant No 60078016) and the Key Research Programme of the National Ministry of Education, China.
†E-mail:GuoHong@phy.ccnu.edu.cn

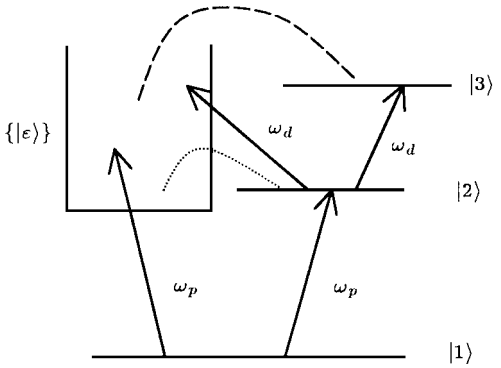


Fig.1. Diagram of the atom–field coupling.

the transition processes $|2\rangle \leftrightarrow |\varepsilon\rangle$ are included. The atomic transitions $|j\rangle \leftrightarrow |\varepsilon\rangle$ (j=2,3) are induced by configuration interactions. In the rotating-wave approximation, the interaction Hamiltonian of the atom–field coupling system in the interaction picture is written as

$$\begin{aligned} V^I(t) =& \Omega_1|2\rangle\langle 1|\mathrm{e}^{\mathrm{i}\Delta_1 t} + \Omega_2|3\rangle\langle 2|\mathrm{e}^{\mathrm{i}\Delta_2 t} \\ &+ \int \mathrm{d}\varepsilon\Omega_{\varepsilon 1}|\varepsilon\rangle\langle 1|\exp[\mathrm{i}(\varepsilon-\omega_p-\omega_1)t] \\ &+ \int \mathrm{d}\varepsilon\Omega_{\varepsilon 2}|\varepsilon\rangle\langle 2|\exp[\mathrm{i}(\varepsilon-\omega_d-\omega_2)t] \\ &+ \int \mathrm{d}\varepsilon\mu_{\varepsilon 2}|\varepsilon\rangle\langle 2|\exp[\mathrm{i}(\varepsilon-\omega_2)t] \\ &+ \int \mathrm{d}\varepsilon\mu_{\varepsilon 3}|\varepsilon\rangle\langle 3|\exp[\mathrm{i}(\varepsilon-\omega_3)t] + \mathrm{h.c}, \quad (1) \end{aligned}$$

where $\Delta_1 = \omega_2 - \omega_1 - \omega_p$ and $\Delta_2 = \omega_3 - \omega_2 - \omega_d$ are the one-photon detunings, Ω_1, Ω_2, $\Omega_{\varepsilon 1}$ and $\Omega_{\varepsilon 2}$ are the matrix elements of the atom–field coupling interactions, and $\mu_{\varepsilon 2}$ and $\mu_{\varepsilon 3}$ represent the strengths of the configuration interactions related to the transitions $|2\rangle \leftrightarrow |\varepsilon\rangle$ and $|3\rangle \leftrightarrow |\varepsilon\rangle$, respectively.

If the atom is initially in its ground state $|1\rangle$, then in the interaction picture the state vector of the atom–field coupling system at time t develops into

$$|\Psi^I(t)\rangle = C_1(t)|1\rangle + C_2(t)\exp(\mathrm{i}\Delta_1 t)|2\rangle + C_3(t)\exp[\mathrm{i}(\Delta_1+\Delta_2)t]|3\rangle + \int \mathrm{d}\varepsilon C_\varepsilon(t)|\varepsilon\rangle, \quad (2)$$

Bringing the Schrödinger equation into the interaction picture and using the Markov approximation and the pole approximation to eliminate $C_\varepsilon(t)$, we obtain that the probability amplitudes $C_j(t)$ (j=1,2,3) for the three bound states $|j\rangle$ obey

$$\mathrm{i}\frac{\mathrm{d}}{\mathrm{d}t}\begin{pmatrix} C_3(t) \\ C_2(t) \\ C_1(t) \end{pmatrix} = \begin{pmatrix} \Delta_1+\Delta_2-\mathrm{i}\Gamma_3 & \sqrt{\Gamma_3 r_2}(q_3-i) & 0 \\ \sqrt{\Gamma_3 r_2}(q_3-i) & \Delta_1-\mathrm{i}(\Gamma_2+r_2) & \sqrt{\Gamma_2 r_1}(q_2-i) \\ 0 & \sqrt{\Gamma_2 r_1}(q_2-i) & -\mathrm{i}r_1 \end{pmatrix}\begin{pmatrix} C_3(t) \\ C_2(t) \\ C_1(t) \end{pmatrix} = V_{\mathrm{eff}}\begin{pmatrix} C_3(t) \\ C_2(t) \\ C_1(t) \end{pmatrix}, \quad (3)$$

where q_2 and q_3 are the Fano asymmetric factors which are associated with the two autoionizing states $|2\rangle$ and $|3\rangle$, respectively, Γ_2 and Γ_3 represent the autoionization widths of the two states $|2\rangle$ and $|3\rangle$, respectively, and r_i denotes the photoionization rate of the state $|i\rangle$ (i=1,2). From Eq.(3) we see that, by eliminating the flat continuum states $\{|\varepsilon\rangle\}$, the atom–field coupling system is effectively identified as a cascade three-level damping system, which is characterized by the non-Hermitian operator V_{eff} defined in Eq.(3).

Taking into consideration the initial condition, the above equation can be solved analytically as

$$\begin{aligned} C_1(t) =& A\left[\frac{(\lambda_1+\Gamma_3+\mathrm{i}\Delta)(\lambda_2-\lambda_3)}{\lambda_1+r_1}\mathrm{e}^{\lambda_1 t}\right. \\ &+ \frac{(\lambda_2+\Gamma_3+\mathrm{i}\Delta)(\lambda_3-\lambda_1)}{\lambda_2+r_1}\mathrm{e}^{\lambda_2 t} \\ &\left.+ \frac{(\lambda_3+\Gamma_3+\mathrm{i}\Delta)(\lambda_1-\lambda_2)}{\lambda_3+r_1}\mathrm{e}^{\lambda_3 t}\right], \end{aligned}$$

$$\begin{aligned} C_2(t) =& -\frac{A}{\sqrt{\Gamma_2 r_1}(1+\mathrm{i}q_2)}[(\lambda_1+\Gamma_3+\mathrm{i}\Delta)(\lambda_2-\lambda_3)\mathrm{e}^{\lambda_1 t} \\ &+ (\lambda_2+\Gamma_3+\mathrm{i}\Delta)(\lambda_3-\lambda_1)\mathrm{e}^{\lambda_2 t} \\ &+ (\lambda_3+\Gamma_3+\mathrm{i}\Delta)(\lambda_1-\lambda_2)\mathrm{e}^{\lambda_3 t}], \end{aligned}$$

$$\begin{aligned} C_3(t) =& \frac{\sqrt{\Gamma_3 r_2}(1+\mathrm{i}q_3)A}{\sqrt{\Gamma_2 r_1}(1+\mathrm{i}q_2)}[(\lambda_2-\lambda_3)\mathrm{e}^{\lambda_1 t} \\ &+ (\lambda_3-\lambda_1)\mathrm{e}^{\lambda_2 t} + (\lambda_1-\lambda_2)\mathrm{e}^{\lambda_3 t}], \quad (4) \end{aligned}$$

with

$$A = \frac{(\lambda_1+r_1)(\lambda_2+r_1)(\lambda_3+r_1)}{(\lambda_2-\lambda_1)(\lambda_3-\lambda_2)(\lambda_1-\lambda_3)(\Gamma_3-r_1+\mathrm{i}\Delta)}, \quad (5)$$

where $\Delta = \Delta_1 + \Delta_2$ is the cascade two-photon detuning, and λ_j (j=1,2,3) are the three roots of the following cubic equation

$$\begin{aligned} &(\lambda+\Gamma_3+\mathrm{i}\Delta)[(\lambda+r_1)(\lambda+\Gamma_2+r_2+\mathrm{i}\Delta_1) \\ &-\Gamma_2 r_1(1+\mathrm{i}q_2)^2] - (\lambda+\mathrm{i}r_1)\Gamma_3 r_2(1+\mathrm{i}q_3)^2 = 0. \quad (6) \end{aligned}$$

3. Photoionization properties of the atom

Now we focus our attention on the properties of the ionization yield. Here we assume that the laser fields will be turned on at time t=0 and last until $t = T$ (square pulses). At the time $t > T$, the ionization yield $Q(t)$ is given by

$$Q(t) = 1 - |C_1(T)|^2 - |C_2(T)|^2 - |C_3(T)|^2. \quad (7)$$

Figure 2 plots the ionization yield $Q(t)$ versus Δ_1 for different q_3. Here we assume that the laser frequency ω_d is fixed, and the laser frequency ω_p is scanned. Figure 2 shows that, with the increase of the Fano asymmetric factor q_3 which is associated with the autoionizing state $|3\rangle$, $Q(t)$ exhibits an asymmetric three-peak distribution versus Δ_1, which is different from the asymmetric two-peak distribution in the Fano autoionization model.[37−39] This is because the model we consider here has two autoionizing states $|2\rangle$ and $|3\rangle$, and the effective interaction Hamiltonian has three complex eigenvalues and three unstable dressed states, among which the interferences result in the appearance of the three-peak distribution in the ionization yield. We also find that, with the increase of q_3, the asymmetric property of the three-peak distribution becomes more distinct. As is known, q_3 just represents the relative intensity between the transition $|2\rangle \leftrightarrow |3\rangle$ and the direct ionization process $|2\rangle \leftrightarrow \{|\varepsilon\rangle\}$. When q_3 is small, i.e. the direct transition process $|2\rangle \leftrightarrow \{|\varepsilon\rangle\}$ is stronger than that of the transition process between the autoionizing states $|2\rangle$ and $|3\rangle$, the difference between the two eigenvalues of the three unstable eigenstates of the atom–field coupling system is small, causing the two peaks in the ionization yield to be nearly coincident with each other. Therefore, the ionization yield exhibits an indistinctive three-peak distribution, as shown in Fig.2(b). In other words, when the atom initially in its ground state $|1\rangle$ is excited to the bound state $|2\rangle$, the ionization possibility of the atom via the direct pathway $|2\rangle \leftrightarrow |\varepsilon\rangle$ is superior to that via the indirect pathway $|2\rangle \leftrightarrow |3\rangle \leftrightarrow \{|\varepsilon\rangle\}$. The effect of the autoionizing state $|3\rangle$ is very weak, so the asymmetric three-peak distribution of $Q(t)$ becomes indistinctive. In contrast, if q_3 is large, corresponding to the condition that the Rabi frequency Ω_2 is large, the differences among the three eigenvalues of $V_{\rm eff}$ are large, and the ionization possibility via the autoionizing state $|3\rangle$ due to the configuration interaction is large, so the distinctive asymmetric three-peak distribution appears in the ionization yield $Q(t)$.

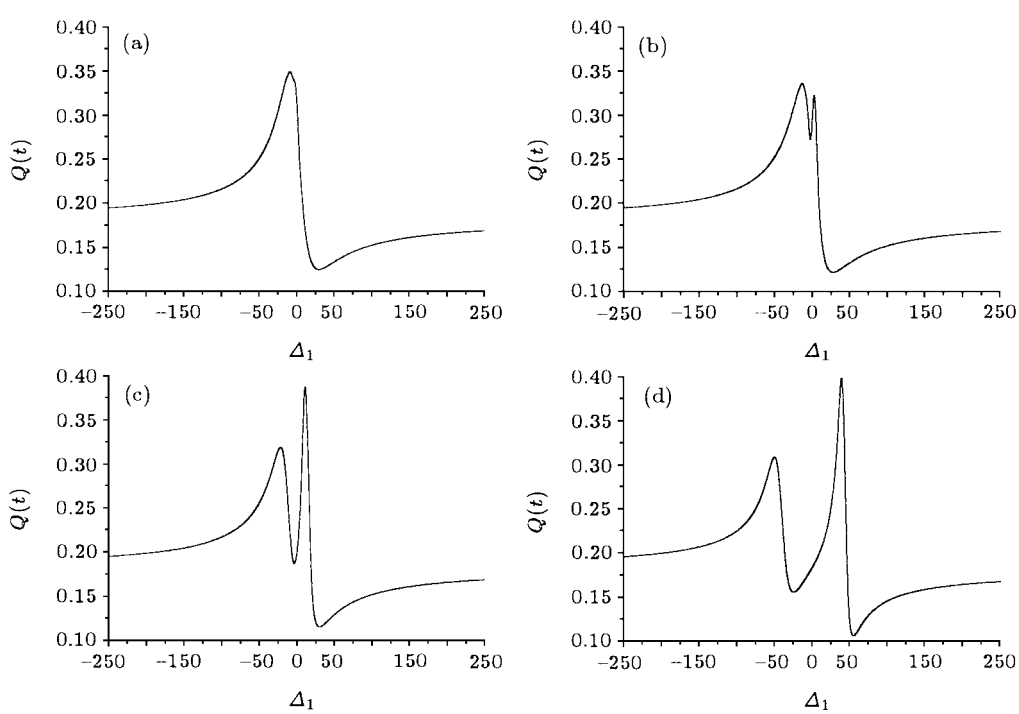


Fig.2. The ionization yield $Q(t)$ against the detuning Δ_1 for different q_3, here q_2=2, Γ_2=5, Γ_3=1, r_2=10, r_1=0.1, Δ_2=0, T=1, and (a) q_3=0.5; (b) q_3=1.5; (c) q_3=4.5; (d) q_3=13.5.

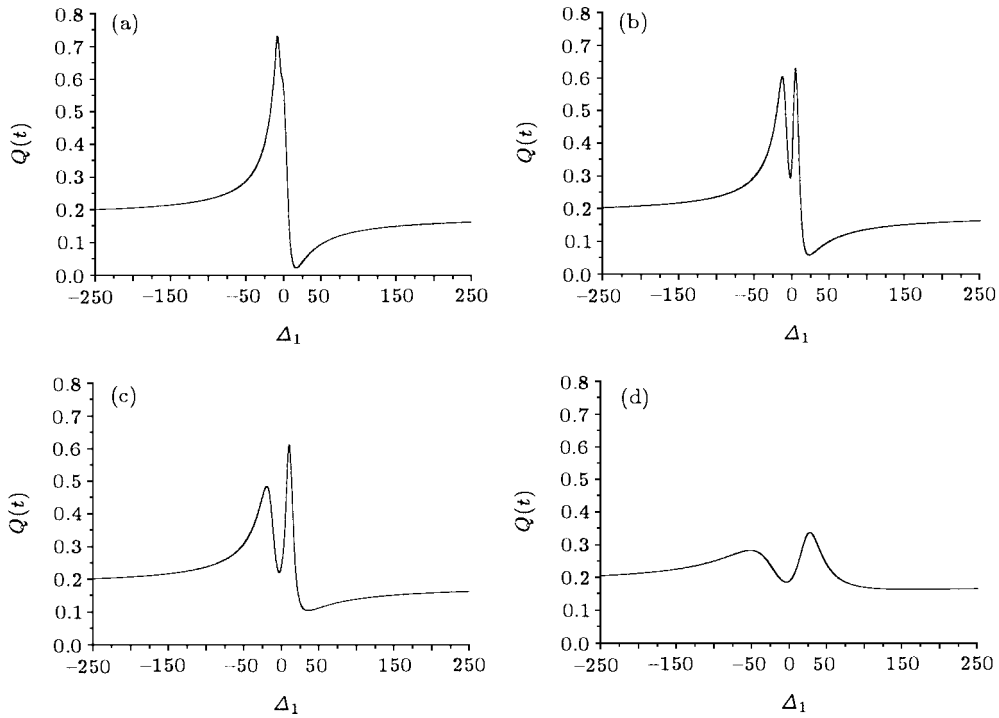


Fig.3. $Q(t)$ versus Δ_1 for different r_2, here q_2=3, q_3=5, Γ_2=5, Γ_3=1, r_1=0.1, Δ_2=0, T=1, and (a) r_2=0.5; (b) r_2=2.5; (c) r_2=7.5; (d) r_2=30.

Figure 3 shows the effect of the photoionization rate r_2 on the line shape of the ionization yield $Q(t)$. We see from Fig.3(a) that the line shape of $Q(t)$ has nearly asymmetric two peaks similar to that in the Fano autoionization model.[37−39] This is because for small r_2, the Rabi frequencies Ω_2 and $\Omega_{\varepsilon 2}$ are very small, such that the effect of the autoionizing state $|3\rangle$ can be neglected, and the atom–field coupling system is reduced to the standard Fano autoionization model. Therefore, one peak in the ionization yield disappears and only two peaks appear in $Q(t)$. With the increase of r_2, the asymmetric three peaks appear in $Q(t)$ since the effects of the autoionizing states $|3\rangle$ must be included. But, for the case of large r_2, we find from Fig.3(d) that the line shape of $Q(t)$ is reduced to a two-peak shape. The reason is that when the atom initially in $|1\rangle$ is excited to $|2\rangle$, the probability of the atom jumping into the continuum $\{|\varepsilon\rangle\}$ due to the interaction with the laser field ω_d is much larger than that of jumping into $\{|\varepsilon\rangle\}$ directly under the configuration interaction between $|2\rangle$ and $\{|\varepsilon\rangle\}$. In this case, the nondegenerate two-photon transition processes play a dominant role in the ionization yield, so the asymmetric two-peak line shape of $Q(t)$ appears again.

Figure 4 illustrates the influence of the one-photon detuning Δ_2 on the ionization yield $Q(t)$. We find that, by increasing Δ_2, the centre of the left peak in $Q(t)$ is shifted to the left side, and the height of this peak is reduced evidently. For the case of large Δ_2, the left peak disappears and $Q(t)$ exhibits an asymmetric two-peak pattern as shown in Fig.4(d). As is known, the photoionization system we consider here is identified as a cascade three-level damping system described by the effective Hamiltonian $V_{\rm eff}$; when the one-photon detuning Δ_2 increases, the probability amplitude of the atom occupying one of the dressed states of $V_{\rm eff}$ decreases, leading to a decrease of the height of the left peak. When Δ_2 becomes very large, the atom excited into the intermediate state $|2\rangle$ jumps into the continuum $\{|\varepsilon\rangle\}$. That is, in the atom–field coupling system, the transition processes $|1\rangle \leftrightarrow |2\rangle \leftrightarrow |\varepsilon\rangle$ are clearly dominant compared to the nondegenerate two-photon processes $|1\rangle \leftrightarrow |2\rangle \leftrightarrow |3\rangle$. In this case, the role of the autoionizing state $|3\rangle$ can be neglected and the system can be identified as a two-level system. Thus, one peak in $Q(t)$ disappears as illustrated in Fig.4(d).

In Fig.5 we show $Q(t)$ for the strong probe case,

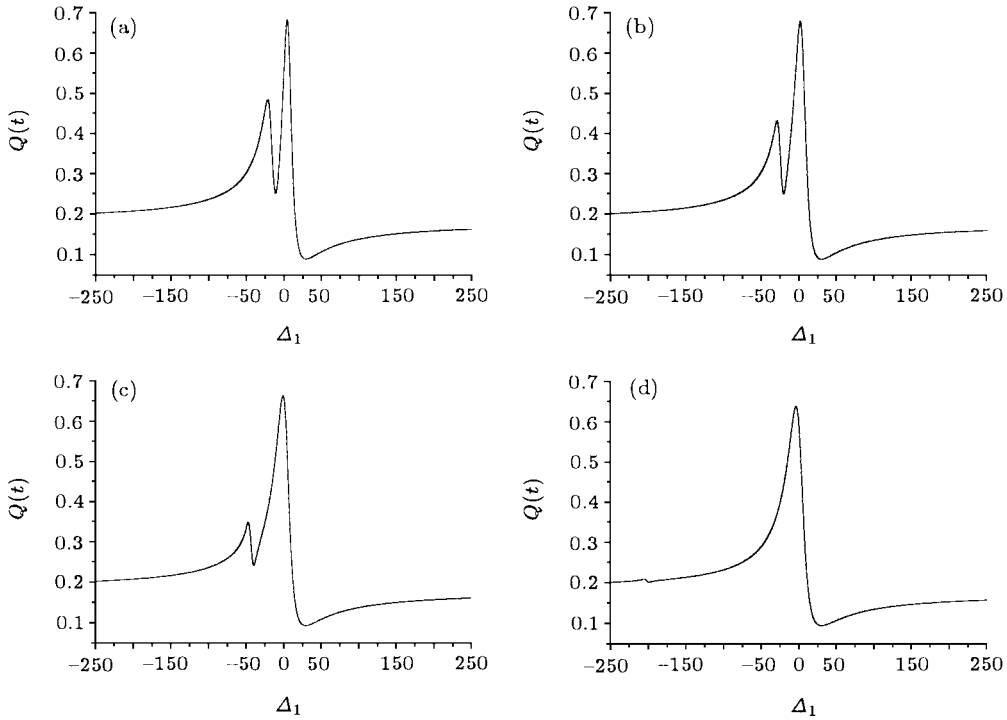


Fig.4. $Q(t)$ versus Δ_1 for different Δ_2, here q_2=3, q_3=5, Γ_2=5, Γ_3=1, r_1=0.1, r_2=5, T=1, and (a) Δ_2=5; (b) Δ_2=15; (c) Δ_2=40; (d) Δ_2=80.

where r_1=1.0. The photoionization line shape changes drastically and becomes a dip, indicating that the atom is partially ionized and the atomic coherent population trapping in bound states occurs. Figure 5 shows that, with increasing r_2, the centre of the dip is shifted to the left side, and the ionization yield increases. In order to make the physical processes transparent, we employ the dressed states to briefly discuss the atomic coherent population trapping. The dressed atomic states $|\psi\rangle$ and the dressed-state energy u of the effective Hamiltonian described by $V_{\rm eff}$ obey

$$V_{\rm eff}|\psi\rangle = u|\psi\rangle. \tag{8}$$

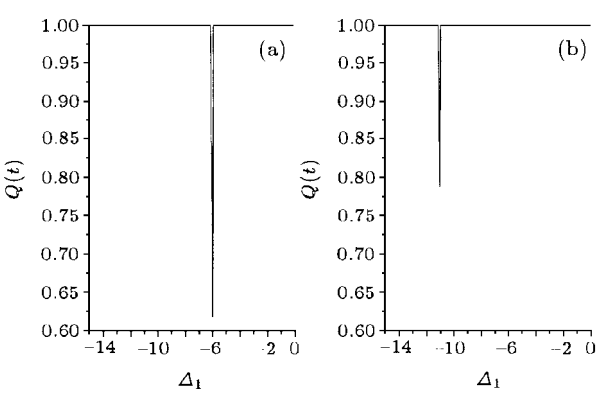


Fig.5. $Q(t)$ versus Δ_1 for r_1=1, Γ_2=5, Γ_3=1, q_3=−5, Δ_2=−5, T=5: (a) r_2=6, q_2=6; (b) r_2=11, q_2=11.

We can see that, in general, the effective system has three unstable eigenstates, corresponding to the atom being ionized completely, so an asymmetric three-peak distribution in $Q(t)$ appears. However, in order to prevent the atom from being ionized completely, one of the eigenvalues u_i (i=1,2,3) must be reduced to a real one, that is to say, the system has one stable eigenstate. It is easy to find that, when Δ_1, Δ_2, q_2, q_3 and r_2 satisfy

$$\begin{aligned}\Delta_1 &= r_2 q_3 + \Gamma_2 q_2 - r_1 q_2,\\ \Delta_2 &= q_3\Gamma_3 - r_2 q_2 - \Gamma_2 q_2,\end{aligned} \tag{9}$$

one of the eigenvalues becomes $u_1 = -q_2 r_1$, and the corresponding stable eigenstate is written as

$$\begin{aligned}|\psi\rangle =& \frac{1}{\sqrt{\Gamma_2\Gamma_3 + r_1\Gamma_3 + r_1 r_2}}\\ &\times\left(\sqrt{\Gamma_2\Gamma_3}\,|1\rangle - \sqrt{r_1\Gamma_3}\,|2\rangle + \sqrt{r_1 r_2}\,|3\rangle\right).\end{aligned} \tag{10}$$

Evidently, we can see that the effects of the coupling between the ground state $|1\rangle$ and the continuum $|\varepsilon\rangle$ are necessary to lead to the atomic coherent population trapping. In this case, if the atom is initially in its ground state $|1\rangle$ and the duration of laser pulses is sufficiently long, then the population trapped in the coherent population trapping state $|\psi\rangle$ is

$$p_t = \frac{\Gamma_2\Gamma_3}{\Gamma_2\Gamma_3 + r_1\Gamma_3 + r_1 r_2}, \tag{11}$$

and the entire trapped population is distributed over the bare atomic states $|1\rangle$, $|2\rangle$ and $|3\rangle$ in the following form

$$P_1 = P_t^2, \quad P_2 = \frac{P_t r_1 \Gamma_3}{\Gamma_2\Gamma_3 + r_1\Gamma_3 + r_1 r_2},$$
$$P_3 = \frac{P_t r_1 r_2}{\Gamma_2\Gamma_3 + r_1\Gamma_3 + r_1 r_2}. \qquad (12)$$

Evidently, with the increase of r_2, the absolute value of q_2 increases in accordance with Eq.(9), so the dip in Fig.5 is shifted towards the left side, and the population trapped in the stable state $|\psi\rangle$ decreases. Figure 5 shows these results exactly. However, from Eq.(12) we find that, with the increase of r_2, although the entire population decreases evidently, the population trapped in the high-lying autoionizing state $|3\rangle$ can exceed that in the ground state $|1\rangle$ when $r_1 r_2 > \Gamma_2\Gamma_3$. In this case, the population inversion occurs.

4. Conclusions

In conclusion, we have studied the photoionization properties of an atom with a ladder coupling scheme involving two autoionizing states coupled to each other. The effects of the coherent coupling between two autoionizing states and between the low-lying autoionizing state and the continuum on the ionization yield are discussed. We find that, when the coupling strength between the two autoionizing states is very weak or very strong, the ionization yield versus the detuning Δ_1 exhibits a dim asymmetric three-peak line shape, or a nearly two-peak line shape. If the coupling strength is chosen moderately, the distinct asymmetric three-peak distribution appears in $Q(t)$. We also find that the coupling between the ground state and the continuum is necessary to lead to the atomic coherent population trapping. The coherent population trapping results in a dipped line shape of $Q(t)$. The coherent population trapping state is the superposition of the ground state and the two autoionizing states. Also, when the laser intensities are chosen appropriately, a population inversion can occur.

References

[1] Shao Y L, Charamlambidis D, Fotakis C, Zhang J and Lambropoulos P 1991 *Phys. Rev. Lett.* **67** 3669
[2] Cavalieri S, Pavone F S and Matera M 1991 *Phys. Rev. Lett.* **67** 3673
[3] Faucher O, Chara-lambidis D, Fotakis C, Zhang J and Lambropoulos P 1993 *Phys. Rev. Lett.* **70** 3004
[4] Faucher O, Shao Y L, Charalambidis D and Fotakis C 1994 *Phys. Rev.* A **50** 641
[5] Cavalieri S, Eramo R and Fini L 1995 *J. Phys. B: At. Mol. Opt. Phys.* **28** 1793
Cavalieri S, Eramo R and Fini L 1995 *J. Phys. B: At. Mol. Opt. Phys.* **28** L637
[6] Li G X and Peng J S 1996 *Phys. Lett.* A **218** 41
[7] Kylstra N J and Joachain C J 1998 *Phys. Rev.* A **57** 412
[8] Li G X, Huang G M and Peng J S 1998 *Acta Phys. Sin.* (Overseas Edition) **7** 422
[9] Magunov A I, Rotter I and Strakhova S I 1999 *J. Phys. B: At. Mol. Opt. Phys.* **32** 1489
[10] Shahriar M S and Hemmer P R 1990 *Phys. Rev. Lett.* **65** 1865
[11] Maichen W, Gaggl R, Kossunsky E and Windholz L 1995 *Europhys. Lett.* **31** 189
[12] Maichen W, Gaggl R, Kossunsky E and Windholz L 1996 *Phys. Rev.* A **53** 3444
[13] Li G X and Peng J S 1996 *Phys. Lett.* A **219** 49
[14] Guo H and Peng J S 2001 *J. Mod. Opt.* **48** 1255
[15] Boller K J, Imamoglu A and Harris S E 1991 *Phys. Rev. Lett.* **66** 2593
[16] Harris S E 1993 *Phys. Rev. Lett.* **70** 552
[17] Harris S E 1994 *Phys. Rev. Lett.* **72** 52
[18] Xiao M, Li Y, Jin S and gea-Bamacloche J 1995 *Phys. Rev. Lett.* **74** 666
[19] Moseley R R, Shepherd S *et al* 1995 *Phys. Rev. Lett.* **74** 670
[20] Marangos J P 1998 *J. Mod. Opt.* **45** 471
[21] Zhao J M 2002 *Chin. Phys.* **11** 241
[22] Harris S E 1989 *Phys. Rev. Lett.* **62** 1033
[23] Zhang J, van Enk S J and Lambropoulos P 1996 *Opt. Commun.* **125** 168
[24] Gaubatz U, Rudecki P, Becker M, Schiemann S, Kulz M and Bergmann K 1988 *Chem. Phys. Lett.* **149** 463
[25] Gaubatz U, Rudecki P, Becker M, Schiemann S, Kulz M and Bergmann K 1990 *J. Chem. Phys.* **92** 5363
[26] Paspalakis E and Knight P L 1998 *J. Phys. B: At. Mol. Opt. Phys.* **31** 2753
[27] Nordam L D, Stapelfeldt H, Duncan D I and Gallagher T F 1992 *Phys. Rev. Lett.* **68** 1496
[28] Jones R R 1995 *Phys. Rev. Lett.* **74** 1091
[29] Jones R R 1995 *Phys. Rev. Lett.* **75** 1491
[30] Jones R R 1996 *Phys. Rev. Lett.* **76** 3927
[31] Li G X and Peng J S 1997 *Opt. Commun.* **138** 59
[32] Parzynski R and Wieczorek S 1998 *Phy. Rev.* A **58** 3051
[33] Guo H and Peng J S 2001 *Acta Opt. Sin.* **21** 410 (in Chinese)
[34] Karapanagioti N E, Faucher O, Shao Y L, Charalambidis D, Bachau H and Cormier E 1995 *Phys. Rev. Lett.* **74** 2431
[35] Karapanagioti N E, Charalambisis D, Uiterwaal C, Fotakis C, Bachau H, Sanchez I and Cormier E 1996 *Phys. Rev.* A **53** 2587
[36] Kylstra N J, van der Hart H W, Burke P G and Joachain C J 1998 *J. Phys. B: At. Mol. Opt. Phys.* **31** 3089
[37] Fano U 1961 *Phys. Rev.* **124** 1866
[38] Nakajima T and Lambropoulos P 1993 *Phys. Rev. Lett.* **70** 1081
[39] Nakajima T and Lambropoulos P 1994 *Phys. Rev.* A **50** 495